

Very fast 2D proton MR spectroscopic imaging of the *in vivo* human brain at 3 Tesla with high spatial resolution using the SSFP based sequence "spectroscopic FAST"

C. Schuster^{1,2}, W. Dreher^{1,2}, and D. Leibfritz^{1,2}

¹University of Bremen, FB 2 (Chemistry), Bremen, Germany, ²Center of Advanced Imaging (CAI), Bremen, Germany

Introduction

In the past, several methods for fast 2D and 3D ¹H MR spectroscopic imaging (MRSI) derived from their corresponding fast MRI methods have been proposed to map the distribution of brain metabolites. Besides echo planar MRSI and spiral MRSI [1-3], various pulse sequences based on the condition of steady state free precession (SSFP) are very promising because of their high signal-to-noise ratio per unit measurement time (SNR_t) and their short minimum measurement time (T_{min}) [4]. To date, only the SSFP based sequences spectroscopic CE-FAST (spCE-FAST) [5] and spectroscopic Missing-Pulse SSFP (spMP-SSFP) [6] have been applied to the *in vivo* human brain at 3 Tesla. Their efficient lipid suppression is essential for *in vivo* measurements to prevent lipid signal contamination of intracranial voxels by voxels from the scalp. In this work, for the first time the SSFP based sequence "spectroscopic FAST" (spFAST) [4] is used for fast 2D ¹H MRSI of the human brain at 3 Tesla. Except for spectroscopic TRUE-FISP [7] with which only single resonances are detectable, spFAST yields the highest possible SNR, among the SSFP based sequences. Therefore, smaller voxel sizes are accessible and thus a higher spatial resolution is achieved within a reasonable measurement time. Although in spFAST the signal intensity of lipids is much higher than the intensity of brain metabolites, contamination of voxels inside the brain by extracranial lipid signals is minimized by spectral-spatial RF excitation pulses and an elliptical k-space sampling scheme with subsequent spatial filtering. Furthermore, a large number of phase encoding steps ensures a better spatial localization of lipid signals in the scalp.

Materials and methods

The spFAST sequence is shown in Fig.1. After RF excitation with spectral-spatial composite pulses [8] (1-τ-1-τ-8-τ-8-τ-1-τ-1; spectral minima appear at 1/τ, τ=2ms) which are simultaneously slice and chemical shift selective (for both water and lipid suppression) and subsequent phase encoding gradients, an FID-like signal is acquired. Afterwards, the phase encoding gradients are compensated for by phase rewinding gradients to maintain the steady state. Prior to the next spectral-spatial composite pulse, the echo-like signal is spoiled by using 2ms gradients with an amplitude of 25 mT/m to avoid interference of the signals.

In Fig.2 the relative signal intensities of metabolites with uncoupled spins, water and lipids are simulated in dependence on the flip angle. Assuming (T₁=1400 ms, T₂=210 ms) for metabolites, (T₁=1200 ms, T₂=90 ms) for water and (T₁=210 ms, T₂=65 ms) for lipids as typical *in vivo* relaxation times at 3 Tesla, the transverse magnetization of lipids is about twice the maximum signal intensity of metabolites which makes an efficient lipid suppression more difficult.

The spFAST sequence was implemented on a 3 Tesla Magnetom Allegra head scanner (Siemens Medical Solutions, Erlangen, Germany) and was applied to phantoms and healthy volunteers. A CP head coil was used for both RF transmission and signal reception. Further measurement parameters were: repetition time (TR) = 72 ms, duration of spectral-spatial composite pulse = 12.4 ms, excitation flip angle α = 20°, field of view (FOV) = 190x220 mm², slice thickness = 20 mm, acquisition bandwidth = 5 kHz, 256 complex data points, elliptical k-space sampling and subsequent spatial filtering with a Hamming function. We used a different number of phase encoding (PE) steps in three consecutive measurements to evaluate different spatial

Fig.1: spectroscopic FAST sequence

resolutions with regard to lipid signal localization and SNR:

- 1) PE steps: 28x32, nominal voxel size: 0.93 cm³, real voxel size: 2.02 cm³ due to elliptical k-space sampling and the spatial filtering, measurement time: 48 sec.
 - 2) PE steps: 42x48, nominal voxel size: 0.41 cm³, real voxel size: 0.83 cm³ due to elliptical k-space sampling and the spatial filtering, measurement time: 1 min 49 sec.
 - 3) PE steps: 56x64, nominal voxel size: 0.23 cm³, real voxel size: 0.47 cm³ due to elliptical k-space sampling and the spatial filtering, measurement time: 3 min 13 sec.
- Postprocessing consisted of spectral apodization with a sine-bell function, zero-filling from 256 to 1024 data points, Fourier transformation and phase correction.

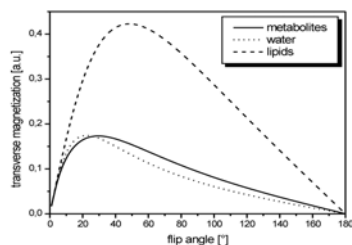


Fig.2: simulation of relative signal intensities with spFAST

Lipid signals were further reduced by the choice of the excitation flip angle of 20°: while the loss of signal intensity for metabolites with uncoupled spins compared to an optimal flip angle of 30° is only 5%, the signal loss of lipids is 21% comparing α = 30° to α = 20°. Further investigations are necessary to empirically adjust TR and the excitation flip angle for maximum SNR_t of metabolites with coupled spins. However, the optimization is hampered because simulation programs for signals of coupled spins are not available yet and signal intensities strongly depend on T₁ and T₂ values which may vary *in vivo*. The short measurement time could be further reduced by an EPI-like readout as done in Ref. 9 for spCE-FAST. In conclusion, the spFAST pulse sequence was successfully implemented at 3 Tesla and provides 2D metabolic maps with a spatial resolution of 0.47 cm³ in about 3 minutes with a high SNR.

Fig.3: T₂-weighted reference image with FOV (white line) and marked voxel position of the spectrum in Fig.4.

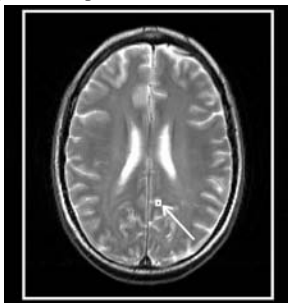


Fig.4: representative spectrum of the 2D MRSI measurement using spFAST with a voxel size of 0.83 cm³

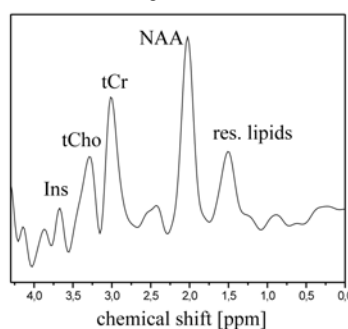
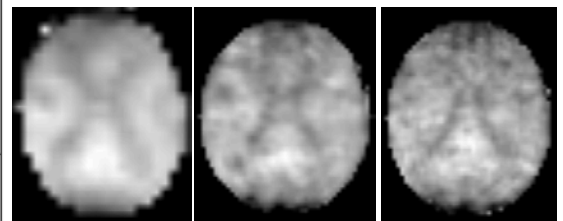


Fig.5: metabolic maps of NAA with different voxel sizes: a) 2.02 cm³ b) 0.83 cm³ c) 0.47 cm³



References

- [1] Chu A et al, Magn Res Med 2003;49:817-821. [2] Ebel A et al, Magn Res Med 2005;53:465-469. [3] Adalsteinsson E et al, Magn Res Med 1998;39:889-898.
- [4] Dreher W et al, Magn Res Med 2003;50:453-460. [5] Geppert C et al, Proc ESMRMB 2005, no.224. [6] Schuster C et al, Proc ISMRM 2006, no.71 and Magn Res Med (in press). [7] Speck O et al, Magn Res Med 2002;48:633-639. [8] Starcuk Z et al, J Magn Res Ser A 1986;66:391-397. [9] Althaus M et al, Magn Res Imag 2006;24:549-555.